



UvA-DARE (Digital Academic Repository)

A measurement of B^0 - anti- B^0 mixing in Z^0 decays

Adeva, B.; Adriani, O.; Aguilar-Benitez, M.; Akbari, H.; Alcaraz, J.; Aloisio, A.; Alverson, G.; Alviggi, M.G.; Linde, F.L.

Published in:
Physics Letters B

DOI:
[10.1016/0370-2693\(90\)90509-5](https://doi.org/10.1016/0370-2693(90)90509-5)

[Link to publication](#)

Citation for published version (APA):

Adeva, B., Adriani, O., Aguilar-Benitez, M., Akbari, H., Alcaraz, J., Aloisio, A., ... Linde, F. L. (1990). A measurement of B^0 - anti- B^0 mixing in Z^0 decays. *Physics Letters B*, 252, 703-712. DOI: 10.1016/0370-2693(90)90509-5

General rights

It is not permitted to download or to forward/distribute the text or part of it without the consent of the author(s) and/or copyright holder(s), other than for strictly personal, individual use, unless the work is under an open content license (like Creative Commons).

Disclaimer/Complaints regulations

If you believe that digital publication of certain material infringes any of your rights or (privacy) interests, please let the Library know, stating your reasons. In case of a legitimate complaint, the Library will make the material inaccessible and/or remove it from the website. Please Ask the Library: <http://uba.uva.nl/en/contact>, or a letter to: Library of the University of Amsterdam, Secretariat, Singel 425, 1012 WP Amsterdam, The Netherlands. You will be contacted as soon as possible.

A measurement of $B^0-\bar{B}^0$ mixing in Z^0 decays

L3 Collaboration

B. Adeva^a, O. Adriani^b, M. Aguilar-Benitez^c, H. Akbari^d, J. Alcaraz^c, A. Aloisio^e, G. Alverson^f, M.G. Alviggi^e, Q. An^g, H. Anderhub^h, A.L. Andersonⁱ, V.P. Andreev^j, T. Angelovⁱ, L. Antonov^k, D. Antreasyan^l, P. Arce^c, A. Arefiev^m, T. Azemoonⁿ, T. Aziz^o, P.V.K.S. Baba^g, P. Bagnaia^p, J.A. Bakken^q, L. Baksay^r, R.C. Ballⁿ, S. Banerjee^{o,g}, J. Bao^d, L. Barone^p, A. Bay^s, U. Beckerⁱ, J. Behrens^h, S. Beingessner^t, Gy.L. Bencze^u, J. Berdugo^c, P. Bergesⁱ, B. Bertucci^p, B.L. Betev^k, A. Biland^h, R. Bizzarri^p, J.J. Blaising^t, P. Blömeke^v, B. Blumenfeld^d, G.J. Bobbink^w, M. Bocciolini^b, W. Böhlen^x, A. Böhm^v, T. Böhringer^y, B. Borgia^p, D. Bourilkov^k, M. Bourquin^s, D. Boutigny^t, B. Bouwens^w, J.G. Branson^z, I.C. Brock^{aa}, F. Bruyant^a, C. Buisson^{ab}, A. Bujak^{ac}, J.D. Burgerⁱ, J.P. Burq^{ab}, J. Busenitz^{ad}, X.D. Cai^g, C. Camps^v, M. Capell^{ae}, F. Carbonara^e, F. Carminati^b, A.M. Cartacci^b, M. Cerrada^c, F. Cesaroni^p, Y.H. Changⁱ, U.K. Chaturvedi^g, M. Chemarin^{ab}, A. Chen^{af}, C. Chen^{ag}, G.M. Chen^{ag}, H.F. Chen^{ah}, H.S. Chen^{ag}, M. Chenⁱ, M.C. Chen^{ai}, M.L. Chenⁿ, G. Chiefari^c, C.Y. Chien^d, F. Chollet^t, C. Civinini^b, I. Clareⁱ, R. Clareⁱ, H.O. Cohn^{aj}, G. Coignet^t, N. Colino^a, V. Commichau^v, G. Conforto^b, A. Contin^a, F. Crijns^w, X.Y. Cui^g, T.S. Daiⁱ, R. D'Alessandro^b, R. de Asmundis^e, A. Degré^{at}, K. Deiters^{a,ak}, E. Dénes^u, P. Denes^q, F. DeNotaristefani^p, M. Dhina^h, D. DiBitonto^{ad}, M. Diemoz^p, F. Diez-Hedo^a, H.R. Dimitrov^k, C. Dionisi^p, F. Dittus^{ai}, R. Dolinⁱ, E. Drago^c, T. Driever^w, D. Duchesneau^s, P. Duinker^{wa}, I. Duran^{ac}, H. El Mamouni^{ab}, A. Engler^{aa}, F.J. Epplingⁱ, F.C. Erné^w, P. Extermann^s, R. Fabbretti^h, G. Faberⁱ, S. Falciano^p, Q. Fan^{g,ag}, S.J. Fan^{al}, M. Fabre^h, O. Fackler^{ae}, J. Fay^{ab}, J. Fehlmann^h, H. Fenker^f, T. Ferguson^{aa}, G. Fernandez^c, F. Ferroni^{pa}, H. Fesefeldt^v, J. Field^s, F. Filthaut^w, G. Finocchiaro^p, P.H. Fisher^d, G. Forconi^s, T. Foreman^w, K. Freudenreich^h, W. Friebel^{ak}, M. Fukushimaⁱ, M. Gailloud^y, Yu. Galaktionov^m, E. Gallo^b, S.N. Ganguli^o, P. Garcia-Abia^c, S.S. Gau^{af}, S. Gentile^p, M. Glaubman^f, S. Goldfarbⁿ, Z.F. Gong^{g,ah}, E. Gonzalez^c, A. Gordeev^m, P. Göttlicher^v, D. Goujon^s, G. Gratta^{ai}, C. Grinnellⁱ, M. Gruenewald^{ai}, M. Guanziroli^g, A. Gurtu^o, H.R. Gustafsonⁿ, L.J. Gutay^{ac}, H. Haan^v, S. Hancke^v, K. Hangarter^v, M. Harris^a, A. Hasan^g, D. Hauschildt^w, C.F. He^{al}, T. Hebbeker^v, M. Hebert^z, G. Hertenⁱ, U. Herten^y, A. Hervé^a, K. Hilgers^v, H. Hofer^h, H. Hoorani^g, L.S. Hsu^{af}, G. Hu^g, G.Q. Hu^{al}, B. Ille^{ab}, M.M. Ilyas^g, V. Innocente^{ca}, E. Isiksal^h, E. Jagel^g, B.N. Jin^{ag}, L.W. Jonesⁿ, R.A. Khan^g, Yu. Kamyshkov^m, Y. Karyotakis^{ta}, M. Kaur^g, S. Khokhar^g, V. Khoze^j, M.-N. Kienzle^s, W. Kinnison^{am}, D. Kirkby^{ai}, W. Kittel^w, A. Klimentov^m, A.C. König^w, O. Kornadt^v, V. Koutsenko^m, R.W. Kraemer^{aa}, T. Kramerⁱ, V.R. Krastev^k, W. Krenz^v, J. Krizmanic^d, A. Kuhn^x, K.S. Kumar^{an}, V. Kumar^g, A. Kunin^m, A. van Laak^v, V. Laliou^s, G. Landi^b, K. Lanus^a, D. Lanske^v, S. Lanzano^c, P. Lebrun^{ab}, P. Lecomte^h, P. Lecoq^a, P. Le Coultre^h, D. Lee^{am}, I. Leedom^f, J.M. Le Goff^a, L. Leistam^a, R. Leiste^{ak}, M. Lenti^b, J. Lettry^h, P.M. Levchenko^j, X. Leytens^w, C. Li^{ah}, H.T. Li^{ag}, J.F. Li^g, L. Li^h, P.J. Li^{al}, Q. Li^g, X.G. Li^{ag}, J.Y. Liao^{al}, Z.Y. Lin^{ah}, F.L. Linde^{aa}, D. Linnhofer^a, R. Liu^g, Y. Liu^g, W. Lohmann^{ak}, S. Lökös^r, E. Longo^p, Y.S. Lu^{ag}, J.M. Lubbers^w, K. Lübelmeyer^v, C. Luci^a, D. Luckey^{li}, L. Ludovici^p, X. Lue^h, L. Luminari^p, W.G. Ma^{ah}, M. MacDermott^h, R. Magahiz^r, M. Maire^t, P.K. Malhotra^o, R. Malik^g, A. Malinin^m, C. Mañá^c, D.N. Maoⁿ,

Y.F. Mao ^{ag}, M. Maolinbay ^h, P. Marchesini ^g, A. Marchionni ^b, J.P. Martin ^{ab}, L. Martinez ^a, F. Marzano ^p, G.G.G. Massaro ^w, T. Matsuda ⁱ, K. Mazumdar ^o, P. McBride ^{an}, T. McMahon ^{ac}, D. McNally ^h, Th. Meinholz ^v, M. Merk ^w, L. Merola ^c, M. Meschini ^b, W.J. Metzger ^w, Y. Mi ^g, M. Micke ^v, U. Micke ^v, G.B. Mills ^{am}, Y. Mir ^g, G. Mirabelli ^p, J. Mnich ^v, M. Möller ^v, B. Monteleoni ^b, G. Morand ^s, R. Morand ^l, S. Morganti ^p, V. Morgunov ^m, R. Mount ^{ai}, E. Nagy ^u, M. Napolitano ^c, H. Newman ^{ai}, M.A. Niaz ^g, L. Niessen ^v, D. Pandoulas ^v, F. Plasil ^{aj}, G. Passaleva ^b, G. Paternoster ^c, S. Patricelli ^c, Y.J. Pei ^v, D. Perret-Gallix ^t, J. Perrier ^s, A. Pevsner ^d, M. Pieri ^b, P.A. Piroué ^q, V. Plyaskin ^m, M. Pohl ^h, V. Pojidaev ^m, N. Produit ^s, J.M. Qian ^{ig}, K.N. Qureshi ^g, R. Raghavan ^o, G. Rahal-Callot ^h, P. Razis ^h, K. Read ^q, D. Ren ^h, Z. Ren ^g, S. Reucroft ^f, O. Rind ⁿ, C. Rippich ^{aa}, H.A. Rizvi ^g, B.P. Roe ⁿ, M. Röhner ^v, S. Röhner ^v, U. Roeser ^{ak}, Th. Rombach ^v, L. Romero ^c, J. Rose ^v, S. Rosier-Lees ^l, R. Rosmalen ^w, Ph. Rosselet ^y, J.A. Rubio ^{ac}, W. Ruckstuhl ^s, H. Rykaczewski ^h, M. Sachwitz ^{ak}, J. Salicio ^{ac}, J.M. Salicio ^c, G. Sanders ^{am}, G. Sartorelli ^{kg}, G. Sauvage ^t, A. Savin ^m, V. Schegelsky ^j, D. Schmitz ^v, P. Schmitz ^v, M. Schneegans ^l, M. Schöntag ^v, H. Schopper ^{ao}, D.J. Schotanus ^w, H.J. Schreiber ^{ak}, R. Schulte ^v, S. Schulte ^v, K. Schultze ^v, J. Schütte ^{an}, J. Schwenke ^v, G. Schwering ^v, C. Sciacca ^e, I. Scott ^{an}, R. Sehgal ^g, P.G. Seiler ^h, J.C. Sens ^w, I. Sheer ^z, V. Shevchenko ^m, S. Shevchenko ^m, X.R. Shi ^{aa}, K. Shmakov ^m, V. Shoutko ^m, E. Shumilov ^m, N. Smirnov ^j, A. Sopczak ^{ai,z}, C. Spartiotis ^d, T. Spickermann ^v, B. Spiess ^x, P. Spillantini ^b, R. Starosta ^v, M. Steuer ^{li}, D.P. Stickland ^q, W. Stoeffl ^{ae}, B. Stöhr ^h, H. Stone ^s, K. Strauch ^{an}, B.C. Stringfellow ^{ac}, K. Sudhakar ^{ov}, G. Sultanov ^a, R.L. Sumner ^q, L.Z. Sun ^{ah}, H. Suter ^h, R.B. Sutton ^{aa}, J.D. Swain ^g, A.A. Syed ^g, X.W. Tang ^{ag}, E. Tarkovsky ^m, L. Taylor ^f, E. Thomas ^g, C. Timmermans ^w, Samuel C.C. Ting ⁱ, S.M. Ting ⁱ, Y.P. Tong ^{af}, F. Tonisch ^{ak}, M. Tonutti ^v, S.C. Tonwar ^o, J. Tóth ^u, G. Trowitzsch ^{ak}, K.L. Tung ^{ag}, J. Ulbricht ^x, L. Urbán ^u, U. Uwer ^v, E. Valente ^p, R.T. Van de Walle ^w, H. van der Graaf ^w, I. Vetlitsky ^m, G. Viertel ^h, P. Vikas ^g, U. Vikas ^g, M. Vivargent ^{li}, H. Vogel ^{aa}, H. Vogt ^{ak}, M. Vollmar ^v, G. Von Dardel ^a, I. Vorobiev ^m, A.A. Vorobyov ^j, An.A. Vorobyov ^j, L. Vuilleumier ^y, M. Wadhwa ^g, W. Wallraff ^v, C.R. Wang ^{ah}, G.H. Wang ^{aa}, J.H. Wang ^{ag}, Q.F. Wang ^{an}, X.L. Wang ^{ah}, Y.F. Wang ^b, Z. Wang ^g, Z.M. Wang ^{g,ah}, J. Weber ^h, R. Weill ^y, T.J. Wenaus ⁱ, J. Wenninger ^s, M. White ⁱ, R. Wilhelm ^w, C. Willmott ^c, F. Wittgenstein ^a, D. Wright ^q, R.J. Wu ^{ag}, S.L. Wu ^g, S.X. Wu ^g, Y.G. Wu ^{ag}, B. Wyslouch ⁱ, Y.D. Xu ^{ag}, Z.Z. Xu ^{ah}, Z.L. Xue ^{al}, D.S. Yan ^{al}, B.Z. Yang ^{ah}, C.G. Yang ^{ag}, G. Yang ^g, K.S. Yang ^{ag}, Q.Y. Yang ^{ag}, Z.Q. Yang ^{al}, C.H. Ye ^g, J.B. Ye ^h, Q. Ye ^g, S.C. Yeh ^{af}, Z.W. Yin ^{al}, J.M. You ^g, M. Yzerman ^w, C. Zaccardelli ^{ai}, L. Zehnder ^h, M. Zeng ^g, Y. Zeng ^v, D. Zhang ^z, D.H. Zhang ^w, Z.P. Zhang ^{ah}, J.F. Zhou ^v, R.Y. Zhu ^{ai}, H.L. Zhuang ^{ag} and A. Zichichi ^{ag}

^a European Laboratory for Particle Physics, CERN, CH-1211 Geneva 23, Switzerland

^b INFN - Sezione di Firenze and University of Florence, I-50125 Florence, Italy

^c Centro de Investigaciones Energeticas, Medioambientales y Tecnologicas, CIEMAT, E-28040 Madrid, Spain

^d Johns Hopkins University, Baltimore, MD 21218, USA

^e INFN - Sezione di Napoli and University of Naples, I-80125 Naples, Italy

^f Northeastern University, Boston, MA 02115, USA

^g World Laboratory, FBLJA Project, CH-1211 Geneva, Switzerland

^h Eidgenössische Technische Hochschule, ETH Zürich, CH-8093 Zurich, Switzerland

ⁱ Massachusetts Institute of Technology, Cambridge, MA 02139, USA

^j Leningrad Nuclear Physics Institute, SU-188 350 Gatchina, USSR

^k Central Laboratory of Automation and Instrumentation, CLANP, Sofia, Bulgaria

^l INFN - Sezione di Bologna, I-40126 Bologna, Italy

^m Institute of Theoretical and Experimental Physics, ITEP, SU-117 259 Moscow, USSR

ⁿ University of Michigan, Ann Arbor, MI 48109, USA

^o Tata Institute of Fundamental Research, Bombay 400 005, India

^p INFN - Sezione di Roma and University of Rome "La Sapienza", I-00185 Rome, Italy

- ^q Princeton University, Princeton, NJ 08544, USA
^r Union College, Schenectady, NY 12308, USA
^s University of Geneva, CH-1211 Geneva 4, Switzerland
^t Laboratoire de Physique des Particules, LAPP, F-74519 Annecy-le-Vieux, France
^u Central Research Institute for Physics of the Hungarian Academy of Sciences, H-1525 Budapest 114, Hungary
^v I. Physikalisches Institut, RWTH, W-5100 Aachen, FRG ¹
 and III. Physikalisches Institut, RWTH, W-5100 Aachen, FRG ¹
^w National Institute for High Energy Physics, NIKHEF, NL-1009 DB Amsterdam, The Netherlands
 and NIKHEF-H and University of Nijmegen, NL-6525 ED Nijmegen, The Netherlands
^x Paul Scherrer Institut (PSI), Würenlingen, Switzerland
^y University of Lausanne, CH-1015 Lausanne, Switzerland
^z University of California, San Diego, CA 92182, USA
^{aa} Carnegie Mellon University, Pittsburgh, PA 15213, USA
^{ab} Institut de Physique Nucléaire de Lyon, IN2P3-CNRS/Université Claude Bernard, F-69622 Villeurbanne Cedex, France
^{ac} Purdue University, West Lafayette, IN 47907, USA
^{ad} University of Alabama, Tuscaloosa, AL 35486, USA
^{ae} Lawrence Livermore National Laboratory, Livermore, CA 94550, USA
^{af} High Energy Physics Group, Taiwan, Rep. China
^{ag} Institute of High Energy Physics, IHEP, Beijing, P.R. China
^{ah} Chinese University of Science and Technology, USTC, Hefei, Anhui 230 029, P.R. China
^{ai} California Institute of Technology, Pasadena, CA 91125, USA
^{aj} Oak Ridge National Laboratory, Oak Ridge, TN 37830, USA
^{ak} High Energy Physics Institute, O-1615 Zeuthen-Berlin, FRG
^{al} Shanghai Institute of Ceramics, SIC, Shanghai, P.R. China
^{am} Los Alamos National Laboratory, Los Alamos, NM 87544, USA
^{an} Harvard University, Cambridge, MA 02139, USA
^{ao} University of Hamburg, W-2000 Hamburg, FRG

Received 1 November 1990

We have observed $B^0-\bar{B}^0$ mixing in $Z^0 \rightarrow b\bar{b}$ decays using hadronic events containing dileptons. The data sample corresponds to 118 200 hadron events at $\sqrt{s} \approx M_Z$. From a fit to the dilepton p and p_\perp spectra, we determine the mixing parameter to be $\chi_B = 0.178^{+0.049}_{-0.040}$.

1. Introduction

Flavor-changing weak interactions are able to transform a neutral meson into its antiparticle, leading to the possibility of flavor oscillations or mixing. This phenomenon is known to occur in the $K^0-\bar{K}^0$ system.

In 1987 evidence was presented by UA1 for a similar effect in the $B^0-\bar{B}^0$ system at the CERN proton-antiproton collider [1]. The charge of the lepton produced in the direct semileptonic decay of the b quark can be used to tag the charge of the quark ($b \rightarrow \ell^-$ and $\bar{b} \rightarrow \ell^+$). Thus, like-sign dileptons can arise from mixing. The large fraction of like-sign events in the UA1

dimuon event sample was interpreted as originating from $B^0-\bar{B}^0$ oscillations.

The mixing parameter χ_B gives the probability that a hadron containing a b quark oscillates into a hadron containing a \bar{b} quark at the time of its decay. Assuming the semileptonic branching ratios for all B hadrons are equal, it can be expressed as

$$\chi_B = f_d \chi_d + f_s \chi_s, \quad (1)$$

where f_d and f_s are the fractions of B_d^0 and B_s^0 produced, and χ_d and χ_s are the mixing parameters for B_d^0 and B_s^0 mesons. This parameter,

$$\chi_B = \frac{\text{Br}(b \rightarrow \bar{B}^0 \rightarrow B^0 \rightarrow \mu^+ + X)}{\text{Br}(b \rightarrow B \rightarrow \mu^+ + X)}, \quad (2)$$

was determined by UA1 to be 0.121 ± 0.047 .

Additional evidence for $B^0-\bar{B}^0$ transitions was pro-

¹ Supported by the German Bundesministerium für Forschung und Technologie.

vided by the ARGUS detector at the DORIS II storage ring [2] and by the CLEO Collaboration at CESR [3]. These observations were based on the study of B mesons produced in $\Upsilon(4S)$ decays, where no B_s are produced. The weighted average of these measurements is $\chi_d = 0.16 \pm 0.04$. Other measurements have been made at PEP which are consistent with the presence of $B^0-\bar{B}^0$ oscillations [4].

In this letter we present the first measurement of $B^0-\bar{B}^0$ mixing performed at $\sqrt{s} \approx M_Z$. We perform a maximum likelihood fit to the p and p_\perp spectra of dileptons observed in hadronic decays of the Z^0 in order to determine the $B^0-\bar{B}^0$ mixing parameter χ_B . The p and p_\perp spectra of leptons in hadronic decays of the Z^0 have already been used to measure the partial width of the Z^0 into $b\bar{b}$ and to determine the $b\bar{b}$ forward-backward asymmetry [5,6]. In this analysis we use dimuons, dielectrons and muon-electron events to select $b\bar{b}$ events in which both B mesons decay semileptonically. The data sample corresponds to 5.5 pb^{-1} collected during a scan of the Z^0 resonance using the L3 detector at LEP. The center-of-mass energies are distributed over the range $88.2 \leq \sqrt{s} \leq 94.2 \text{ GeV}$.

2. The L3 detector

The L3 detector covers 99% of 4π . The detector consists of a central tracking chamber, a high resolution electromagnetic calorimeter composed of BGO crystals, a ring of scintillation counters, a uranium and brass hadron calorimeter with proportional wire chamber readout, and a precise muon chamber system. These detectors are installed in a 12 m diameter magnet which provides a uniform field of 0.5 T along the beam direction.

The central tracking chamber is a time expansion chamber which consists of 2 cylindrical layers of 12 and 24 sectors, with 62 wires measuring the $R-\phi$ coordinate. The average single wire resolution is $58 \mu\text{m}$ over the entire cell. The double-track resolution is $640 \mu\text{m}$. The fine segmentation of the BGO detector and the hadron calorimeter allow us to measure the direction of jets with an angular resolution of 2.5° , and to measure the total energy of hadronic events from Z^0 decay with a resolution of 10.2%. The muon detector consists of 3 layers of precise drift chambers, which

measure a muon's trajectory 56 times in the bending plane, and 8 times in the non-bending direction.

For the present analysis, we use the data collected in the following ranges of polar angles:

- for the central chamber, $41^\circ < \theta < 139^\circ$,
- for the hadron calorimeter, $5^\circ < \theta < 175^\circ$,
- for the muon chambers, $35.8^\circ < \theta < 144.2^\circ$,
- for the electromagnetic calorimeter, $42.4^\circ < \theta < 137.6^\circ$.

A detailed description of each detector subsystem, and its performance, is given in ref. [7].

3. Selection of $b\bar{b}$ events

Events of the type $Z^0 \rightarrow b\bar{b}$ are identified by the observation of leptons coming from the semileptonic decay of the b or \bar{b} quark. In order to identify both B hadrons, we look for hadronic events containing at least two leptons (muons or electrons).

These events are triggered by several independent triggers. The primary trigger requires a total energy of 15 GeV in the BGO and hadron calorimeters. A second trigger for inclusive muon events requires one of sixteen scintillation counter ϕ sectors in coincidence with a track in the muon chambers. These triggers, combined with an independent charged track trigger and a barrel scintillation counter trigger, give a trigger efficiency greater than 99.9% for hadronic events, including those containing one or more leptons.

In this analysis we first select hadronic events using the following criteria:

- (1) $E_{\text{cal}} > 38 \text{ GeV}$,
- (2) longitudinal energy imbalance: $|E_\parallel|/E_{\text{vis}} < 0.4$,
- (3) transverse energy imbalance: $E_\perp/E_{\text{vis}} < 0.5$,

where E_{cal} is the total energy observed in the calorimeters, and E_{vis} is the sum of the calorimetric energy and the energy of the muon as measured in the muon chambers.

The number of jets is found using a two-step algorithm which groups the energy deposited in the BGO crystals and in the hadron calorimeter towers into clusters, before collecting the clusters into jets [8]. We require that there be at least one jet which has more than 10 GeV in the calorimeters.

The clustering algorithm normally reconstructs one cluster in the BGO for each electron or photon

shower, and a few clusters for τ 's. We reject $\tau^+\tau^-$ events by requiring a minimum of 10 clusters in the BGO, each with energy greater than 100 MeV.

A total of 118 200 hadronic events were collected during the scan of the Z^0 in the 1989 and 1990 running periods. For the inclusive electron analysis only the data from 1990 is used, which corresponds to 104 400 hadronic events.

Muons are identified and measured in the muon chamber system. We require that a muon track consists of track segments in two of three layers of muon chambers, and that the muon track points to the interaction region. We make the additional requirement that the transverse distance of closest approach of the muon track is less than 3σ from the vertex, and that the longitudinal distance of closest approach is less than 4σ . The effects of multiple scattering of the muon in the calorimeters are included in the errors. In order to be used in this analysis, the momentum of the muon must be larger than 4 GeV. Charge confusion is negligible for muon candidates in this sample ($\ll 1\%$).

We identify electrons in a two-step process, first finding electromagnetic clusters in the BGO calorimeter and then associating them with a charged track. To identify an electromagnetic cluster in a hadronic environment, we look for an energy cluster in the BGO calorimeter which contains at least 9 adjacent crystals each with more than 10 MeV. We then compute the ratio of the energy measured in the 3×3 array centered on the most energetic crystal and the energy measured in the 5×5 array, E_9/E_{25} , where both energy measurements have a position-dependent leakage correction applied. For an isolated electromagnetic shower, E_9/E_{25} has an approximately gaussian distribution, centered at 1.0 with a width of 1%. For hadronic showers, or for electromagnetic showers that have been contaminated by a nearby shower, E_9/E_{25} will be smaller than 1.0. We reject those clusters with E_9/E_{25} less than 0.95. To further reduce the background from pions and kaons misidentified as electrons, we exclude any BGO cluster when there is more than 3 GeV of energy deposited in the hadron calorimeter behind the cluster inside a cone of half-angle 7° around its centroid.

To identify the electromagnetic cluster as an electron, we require a match within 5 mrad in the azimuthal angle between the centroid of the electromag-

netic shower and a track in the central tracking chamber. The charge of the electron is measured in the tracking chamber. Tracks going through lower resolution regions adjacent to the anode and cathode planes are excluded to avoid charge confusion. In addition, we reject those tracks with a measured momentum transverse to the beam direction larger than 35 GeV. Fig. 1 shows the ratio of the electromagnetic energy measured in the calorimeter and the signed momentum measured in the tracking chamber (qE/p) for electron candidates passing the above cuts. Two well-separated peaks are visible at ± 1 . The upper limit of the charge confusion is 1%. The tails at large E/p are due to energetic photons and π^0 's that have been matched to a nearby track. We reject this background by requiring $E/p < 1.5$. We further require that the energy of the electron candidate be greater than 3 GeV.

As an example, fig. 2 shows a hadronic event containing a high momentum electron and a high momentum muon. Both leptons come from the interaction region and have positive charge.

To simulate inclusive dilepton events, we use the Lund parton shower program JETSET 7.2 [9] with $A_{LL} = 290$ MeV and string fragmentation. For b and c quarks we use the Peterson fragmentation function [10]. The b-quark fragmentation function is ad-

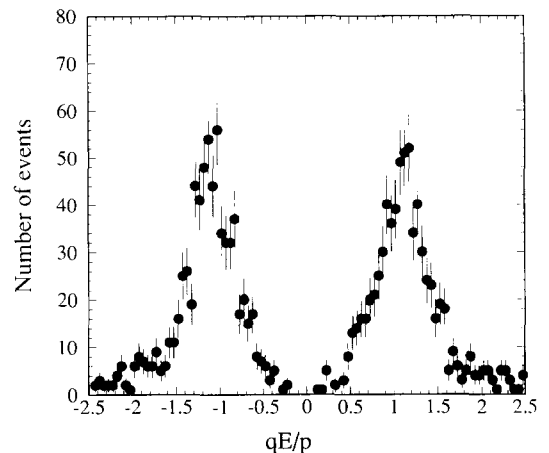


Fig. 1. The ratio of the energy measured in the calorimeter and the signed momentum measured in the central tracking chamber (qE/p) for electron candidates. The tails at large values of E/p are due to energetic photons and π^0 's that have been matched to a nearby track.

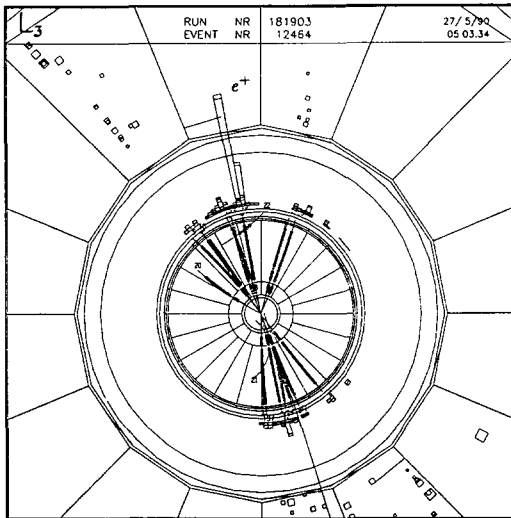
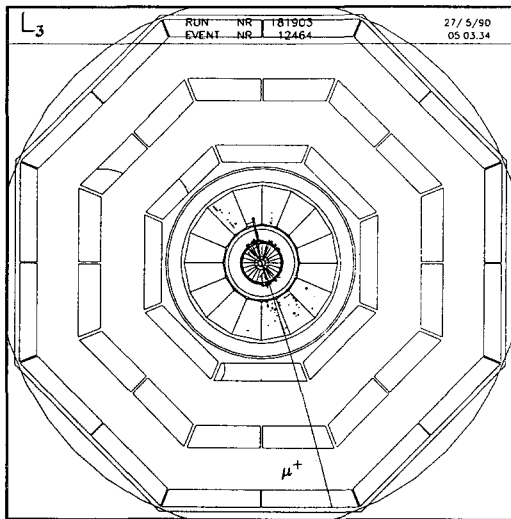


Fig. 2. A hadronic event with like-sign leptons. Both figures show the r - ϕ projection of the event. The muon track can be seen in the upper figure where it is reconstructed in three layers of chambers. In the lower figure a close-up of the BGO calorimeter and TEC chamber shows the electron candidate as the large cluster in the BGO. The size of the symbols indicating individual calorimeter hits corresponds to the magnitude of the energy deposition in that hit. Note that the electron candidate has only one track associated with it and no energy in the hadron calorimeter. The electron has an energy 14 GeV and a p_{\perp} of 2.7 GeV, the muon has a momentum of 17 GeV and a p_{\perp} of 1.7 GeV.

justed to match our inclusive muon data [5]. The generated events are passed through the L3 detector simulation^{#1} which includes the effects of energy loss, multiple scattering, interactions and decays in the detector materials. We use the average of the semileptonic branching ratios measured by previous experiments^{#2}. $\text{Br}(b \rightarrow \mu) = (11.8 \pm 1.1)\%$, and $\text{Br}(c \rightarrow \mu) = (8.0 \pm 1.0)\%$. These branching ratios are also used for $b \rightarrow e$ and $c \rightarrow e$.

4. B^0 - \bar{B}^0 mixing sample

The signature for B^0 - \bar{B}^0 mixing in inclusive lepton events is an event with two leptons of the same charge on opposite sides of the event. The leptons are considered to be on opposite sides when the angle between them is greater than 60° . The major background comes from $Z^0 \rightarrow b\bar{b}$ events, where one b decays into a prompt lepton $b \rightarrow \ell^-$, and the second decays via the cascade $\bar{b} \rightarrow \bar{c} \rightarrow \ell^-$, giving like-sign leptons. Because of the hard fragmentation and large mass of the b quark, the leptons from its semileptonic decay have large momentum p and large transverse momentum p_{\perp} . These features can be used to identify prompt leptons from B -hadron decays. Fig. 3 shows the minimum of the two momenta for the leptons in the inclusive dilepton events which have passed the selection cuts given above. Fig. 4 shows the measured minimum transverse momentum with respect to the nearest jet, p_{\perp} , of each dilepton pair. In defining the axis of the nearest jet, the measured energy of the lepton is first excluded from the jet. The fraction of events with two leptons from prompt $b \rightarrow \ell$ decay increases at higher p and p_{\perp} . Therefore, events with opposite side, high momentum and high p_{\perp} leptons are most probably from prompt $b \rightarrow \ell$ decays. The observation of such events with like-sign leptons is indicative of B^0 - \bar{B}^0 mixing.

A summary of the dilepton data sample is given in table 1. The smaller number of events with electrons is due to the necessity of using strong isolation re-

^{#1} The L3 detector simulation is based on GEANT Version 3.13 (September 1989) [11]. Hadronic interactions are simulated using the GHEISHA program [12].

^{#2} The semileptonic branching ratios are taken from PEP and PETRA data, see ref. [13].

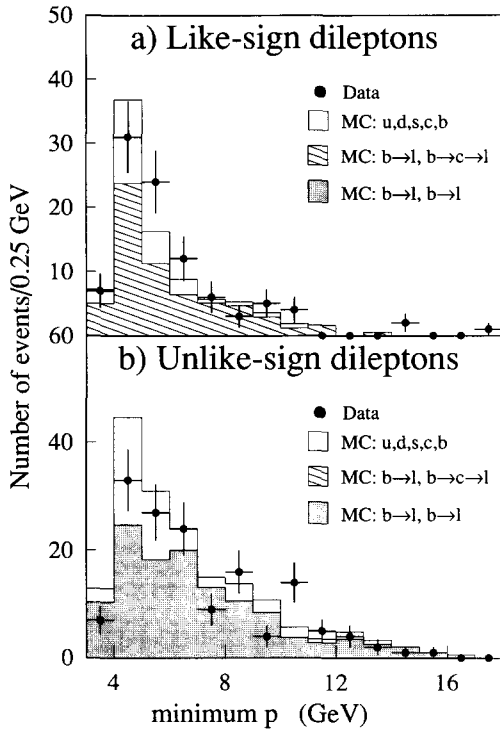


Fig. 3. The distribution of the minimum of the two momenta for (a) like-sign dileptons and (b) unlike-sign dileptons compared to the Monte Carlo simulation with $\chi_B=0$. No p_{\perp} cut has been applied. The shaded region includes $b \rightarrow \ell$, $b \rightarrow \ell$ and $b \rightarrow c \rightarrow \ell$, $b \rightarrow c \rightarrow \ell$ events. The hatched region includes $b \rightarrow \ell$, $b \rightarrow c \rightarrow \ell$ events.

quirements to extract a clean electron sample in the presence of the hadronic background. The excess of $\mu^+\mu^+$ events compared to $\mu^-\mu^-$ events arises from the difference in the punch-through for positive and negative charged particles. Also shown are the number of events passing high p_{\perp} cuts, which select preferentially $b \rightarrow \ell$, $b \rightarrow \ell$ events. In this selection, we require that electrons have $p_{\perp} > 1.0$ GeV and muons have $p_{\perp} > 1.5$ GeV and the two leptons are on opposite sides of the event.

To distinguish mixing events from background, lepton candidates can be classified into five categories:

- (1) Prompt $b \rightarrow \ell$. Included in the prompt $b \rightarrow \ell$ category are events with leptons from the cascades $b \rightarrow \tau \rightarrow \ell$, and $b \rightarrow c \rightarrow \bar{c} + s$ where $\bar{c} \rightarrow \ell$. These cascades yield a lepton with the same sign as direct $b \rightarrow \ell$ decays.
- (2) Cascade $b \rightarrow c \rightarrow \ell$,
- (3) $b \rightarrow$ background coming from B-hadron decay.

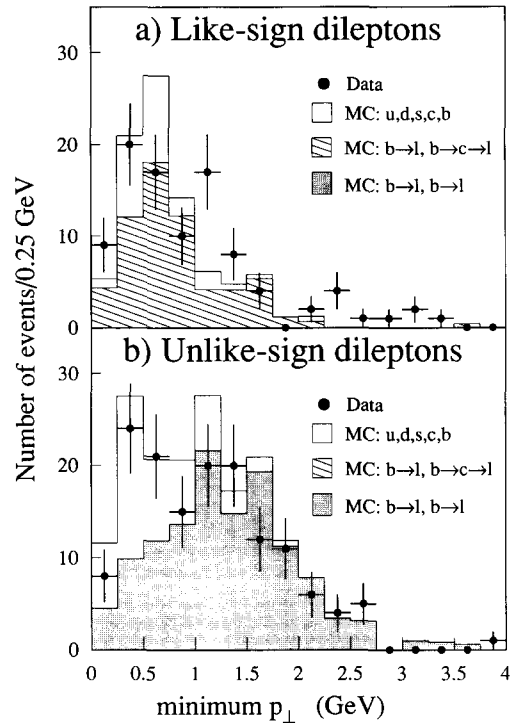


Fig. 4. The distribution of the minimum of the two transverse momenta for the leptons in the inclusive dilepton events compared to the Monte Carlo simulation with $\chi_B=0$ for (a) like-sign dileptons and (b) unlike-sign dileptons.

Table 1
Dilepton events in the data.

Data type	$\ell^+\ell^-$	$\ell^+\ell^+$	$\ell^-\ell^-$	Total
all $\mu\mu$ events	155	50	24	229
high- p_{\perp} $\mu\mu$ events	22	3	4	29
all ee events	17	1	3	21
high- p_{\perp} ee events	6	1	2	9
all μe events	68	26	17	111
high- p_{\perp} μe events	20	3	7	30

- (4) Prompt $c \rightarrow \ell$.

(5) Other backgrounds arising from $udsc \rightarrow$ background and from fragmentation effects in $b\bar{b}$ events.

Background processes include: leptons from π and K decays, hadrons misidentified as electrons, punch-through, Dalitz decay and $\pi-\gamma$ overlap for electrons. Leptons from J decay contribute to 2% of the dilepton sample, but only 0.9% in the high p_{\perp} sample, and

Table 2

Monte Carlo estimates of the fractions (in %) of various categories of dilepton events in the data sample. Since, in the presence of mixing, all charge combinations are possible, we omit the \pm superscripts on the leptons.

Lepton pair category	$p_{\perp} > 0$	High- p_{\perp}
b \rightarrow ℓ , b \rightarrow ℓ	36	80
b \rightarrow c \rightarrow ℓ , b \rightarrow c \rightarrow ℓ	2	3
b \rightarrow ℓ , b \rightarrow c \rightarrow ℓ	32	10
b \rightarrow ℓ , b \rightarrow background	12	4
c \rightarrow ℓ , c \rightarrow ℓ	6	0
others	12	3

have a negligible effect on our measurement.

Table 2 shows the results of Monte Carlo studies giving the fraction of each source of prompt dileptons and of background for data samples with no cut on p_{\perp} , and also with the high- p_{\perp} requirement already described. These p_{\perp} cuts correspond to prompt b \rightarrow ℓ probabilities for electrons and muons of about 80%. The high- p_{\perp} sample can be used to estimate the $B^0 - \bar{B}^0$ mixing by simple event counting.

Using the data in table 1, we compute the ratio $N^{\pm\pm}/N^{+-}$ for opposite-side, high- p_{\perp} events to be 0.42 ± 0.11 while in the Monte Carlo (with $\chi_B = 0$) we find 0.15 ± 0.05 . Subtracting backgrounds estimated from Monte Carlo, and inserting our estimates of the fractions of various dilepton categories, we determine $\chi_B = 0.13 \pm 0.05$ where the error is statistical only. Thus we observe clear evidence for $B^0 - \bar{B}^0$ mixing from simple event counting alone.

The simple counting procedure weights all events equally, however at very large p and p_{\perp} there is almost no background. We use a fitting procedure which gives events with two high- p and $-p_{\perp}$ leptons larger weights than events with low- p or $-p_{\perp}$. By using this fit to determine χ_B we are able to make use of all of the data and also increase our sensitivity to mixing.

5. Determination of χ_B

We perform an unbinned maximum likelihood fit to the p and p_{\perp} distributions for dilepton events in the data to determine the mixing parameter χ_B . To define the probability that the data events contain two b \rightarrow ℓ decays, we use fully simulated Lund five-flavor Monte Carlo events, and also fully simulated and

generator level b-flavor events, where one of the b quarks is forced to decay semileptonically into μ or e. The generator level events are smeared to take into account detector effects.

The likelihood function is determined from the number and type of the Monte Carlo leptons found within a rectangular box centered on each data lepton in $(p_1, p_{\perp 1}, p_2, p_{\perp 2})$ space. We allow the size of the box to increase until a minimum number of 40 Monte Carlo leptons are included. The likelihood function (L) has the form

$$L = \prod_{i=1}^{N_{\text{data}}} \frac{1}{V_{\text{box}}(i)} \sum_{k_1, k_2} N_{k_1, k_2}(i) W_{k_1, k_2}(i) . \quad (3)$$

The index k indicates the category of the lepton source type, $N_k(i)$ is the number of simulated Monte Carlo leptons of this type found in the box with data lepton i , and $V_{\text{box}}(i)$ is the volume of the box. Even with large Monte Carlo statistics, the four dimensional space is sparsely populated in the region of interest, where both leptons have high p and high p_{\perp} . Hence, each box can become large. Therefore, the relative weight of each Monte Carlo event in the box is calculated assuming exponential distributions in p and p_{\perp} . The Monte Carlo events are generated with no mixing, $\chi_B = 0$, and must be reweighted assuming that a fraction χ_B of the leptons from B-hadrons will change sign. After taking mixing into account, only Monte Carlo events which *could* have the same product of lepton charges ($q_1 q_2$) as the data event, and have the same topology (same-side or opposite-side dileptons) contribute to the likelihood function.

For dileptons of category k_1 and k_2 , the weighting function is written as

$$W_{k_1, k_2}(i) = (1 - \chi_{k_1})(1 - \chi_{k_2}) + \chi_{k_1} \chi_{k_2} \quad (4)$$

when the Monte Carlo event and data event have the same product of lepton charges, i.e. $(q_1 q_2)^{\text{MC}} = (q_1 q_2)^{\text{Data}}$. This weight reflects the probability that neither or both leptons carry the same charge as their original parent quark.

The amount of mixing, χ_k , for each category is given by

$$\begin{aligned} \chi_1 &= \chi_B, & \text{for b} \rightarrow \ell, \\ \chi_2 &= \chi_B, & \text{for b} \rightarrow \text{c} \rightarrow \ell, \\ \chi_3 &= 0.5\chi_B, & \text{for b} \rightarrow \text{B-hadron} \rightarrow \text{background} \end{aligned}$$

$$\begin{aligned}\chi_4 &= 0, & \text{for } c \rightarrow \ell, \\ \chi_5 &= 0, & \text{for other backgrounds.}\end{aligned}$$

From Monte Carlo studies we observe that the effective χ is less than χ_B for category 3, (backgrounds arising from B-hadron decays), even though at production the lepton candidates from this source do change sign with mixing. This is largely because many more of the K^- than K^+ are absorbed in the calorimeters.

When the Monte Carlo and the data have different charge products, we calculate the probability that mixing will cause the sign of one lepton to change. When the leptons are in opposite hemispheres, and $(q_1 q_2)^{MC} \neq (q_1 q_2)^{Data}$, the weight is

$$W_{k_1, k_2}(i) = \chi_{k_1}(1 - \chi_{k_2}) + (1 - \chi_{k_1})\chi_{k_2}. \quad (5)$$

When the two data leptons are on the same side and both Monte Carlo leptons originate from the same b hadron, there is no sensitivity to χ , thus

$$W_{k_1, k_2}(i) = 0. \quad (6)$$

From the fit, we determine the mixing parameter,

$$\chi_B = 0.178_{-0.040}^{+0.049},$$

where the error is statistical only. The change in the logarithm of the likelihood function between this value and $\chi_B = 0$ is 32.3, or 8.0 standard deviations.

Table 3 lists the contributions to the systematic error in this measurement. We have estimated the error by changing several parameters by one standard deviation or more of their known (or estimated) uncertainties. We have estimated the contribution from reconstruction errors by an additional smearing of the p_\perp of each data lepton. The error coming from the uncertainty in assigning probabilities to events has been estimated by changing the number of leptons required in the fit box (in the range 20 to 90), as well as using different samples of Monte Carlo events. The combined systematic error on χ_B is estimated to be 0.02.

We have also performed a fit for χ_B with a $p_\perp > 1.0$ GeV cut. This reduces the statistics but also the background substantially, yet changes χ_B by only -0.02 . Although this sample contains the same high- p and $-p_\perp$ events as our result, the low- p_\perp events have been removed, thus it cannot be used as an estimate of the

Table 3
Systematic checks in the χ_B measurement.

Contribution	Error
changing the $b \rightarrow \ell$ and $c \rightarrow \ell$ branching ratios by their associated errors	0.0015
variation of the background fraction by $\pm 15\%$	0.0005
variation of the b fragmentation parameter ϵ_b by $\pm 50\%$	0.0005
changing the definition of opposite side from 45° to 90°	0.003
smearing of the lepton transverse momentum by $\Delta p_\perp / p_\perp = 25\%$	0.005
introduction of an additional charge confusion of 0.5%	0.01
variation of the background mixing dependence, $0.25 < \chi_3 / \chi_B < 1.0$	< 0.0005
variation of the exponential weighting of the p and p_\perp distributions within a box	0.007
probability assignment	0.01

systematic uncertainty, but does verify that the higher backgrounds at low p_\perp are not influencing the result.

As an additional check, a different method is used to measure the mixing parameter using the dileptons. In this method, probability functions are assumed to factorize, and are therefore evaluated independently (using the single lepton data and Monte Carlo) for each lepton as a function of p_L and p_\perp , where p_L is the lepton momentum along the jet axis. This method requires much smaller Monte Carlo statistics, but does not take into account correlations between the lepton momenta. We find $\chi_B = 0.14 \pm 0.04$ where the error is statistical only, in good agreement with the other analysis.

6. Discussion

We can use our measurement of χ_B , along with the combined ARGUS and CLEO value for χ_d , to obtain information on χ_s . Since χ_d has been measured to be large, 0.16 ± 0.04 , in the standard model the $B_s^0 - \bar{B}_s^0$ mixing is expected to be maximal, i.e. $\chi_s \approx 0.5$. Assuming that the relative abundances of B_d and B_s mesons at LEP energies are given by $f_d = 0.375$ and $f_s = 0.15$ [14]; we show in fig. 5 a plot in the $\chi_d - \chi_s$ plane corresponding to our measurement. Also shown in the figure is the ARGUS/CLEO value for χ_d .

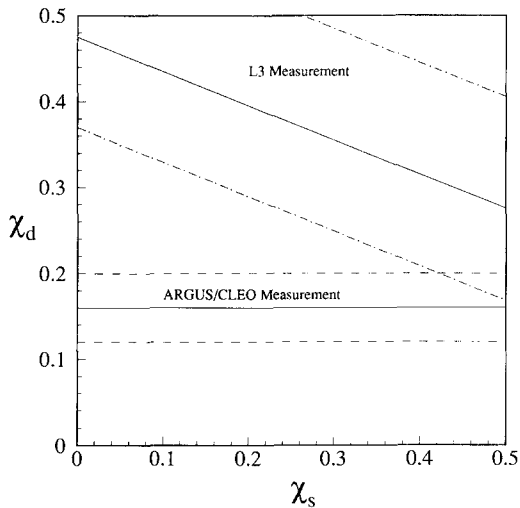


Fig. 5. A comparison of our $B^0-\bar{B}^0$ mixing results with those from ARGUS and CLEO. $f_d=0.375$ and $f_s=0.15$ is assumed, where $\chi_B=f_d\chi_d+f_s\chi_s$. The dashed and dot-dashed lines correspond to the 1 standard deviation limits in both cases.

Combining our result with that of ARGUS/CLEO and taking into account possible variations in the f_d and f_s parameters of up to 0.05, we obtain a value of $\chi_s=0.79^{+0.47}_{-0.34}$. Because χ_s must lie in the range $0\leq\chi_s\leq 0.5$, the classical statistical technique for computing a lower limit on χ_s cannot be used. We compute a 90% lower limit of $\chi_s>0.14$ with respect to the integral of the probability distribution between 0.0 and 0.5 [15].

7. Conclusions

We have measured mixing in the $B^0-\bar{B}^0$ system using inclusive dilepton events from approximately 118 000 Z^0 decays. The uncertainty in χ_B is domi-

nated by the statistics. We determine the $B^0-\bar{B}^0$ mixing parameter to be $\chi_B=0.178^{+0.049}_{-0.040}$, which is 8 standard deviations from zero. Our result is consistent with maximal mixing in the $B_s^0-\bar{B}_s^0$ system as expected in the standard model.

References

- [1] UA1 Collab., C. Albajar et al., Phys. Lett. B 186 (1987) 27; B 197 (1987) 565 (E).
- [2] ARGUS Collab., H. Albrecht et al., Phys. Lett. B 192 (1987) 245.
- [3] CLEO Collab., M. Artuso et al., Phys. Rev. Lett. 62 (1989) 2233.
- [4] MAC Collab., H. Band et al., Phys. Lett. B 200 (1988) 221; MARK II Collab., A.J. Weir et al., Phys. Lett. B 240 (1990) 289.
- [5] L3 Collab., B. Adeva et al., Phys. Lett. B 241 (1990) 416.
- [6] ALEPH Collab., D. Decamp et al., Phys. Lett. B 244 (1990) 551; MARK II Collab., J.F. Kral et al., Phys. Rev. Lett. 64 (1990) 1211.
- [7] L3 Collab., B. Adeva et al., Nucl. Instrum. Methods A 289 (1990) 35.
- [8] O. Adriani et al., Hadron calorimetry in the L3 detector, Nucl. Instrum. Methods, to be published.
- [9] T. Sjöstrand and M. Bengtsson, Comput. Phys. Commun. 43 (1987) 367; T. Sjöstrand, in: Z physics at LEP, CERN report CERN-89-08, Vol. III, p. 143.
- [10] C. Peterson et al., Phys. Rev. D 27 (1983) 105.
- [11] See R. Brun et al., GEANT 3, CERN report DD/EE/84-1 (revised) (September 1987).
- [12] See H. Fesefeldt, RWTH Aachen preprint PITHA 85/02 (1985).
- [13] JADE Collab., W. Bartel et al., Z. Phys. C 33 (1987) 339, and references therein.
- [14] J. Kühn and P. Zerwas, Heavy flavors at LEP, preprint MPI-PAE/PTh 49/89.
- [15] Particle Data Group, J.J. Hernández et al., Review of particle properties, Phys. Lett. B 239 (1990) III.35.